Spring 2013

A computational study of thermal storage techniques for solar cooking devices for use in Rajasthan, India

Scott James Ruebush
University of Iowa

A COMPUTATIONAL STUDY OF THERMAL STORAGE TECHNIQUES FOR SOLAR COOKING DEVICES FOR USE IN RAJASTHAN, INDIA

by

Scott James Ruebush

A thesis submitted in partial fulfillment of the requirements for the Master of Science degree in Mechanical Engineering in the Graduate College of The University of Iowa

May 2013

Thesis Supervisor: Professor H.S. Udaykumar

Graduate College
The University of Iowa
Iowa City, Iowa

CERTIFICATE OF APPROVAL

_____

MASTER'S THESIS

_____

This is to certify that the Master's thesis of

Scott James Ruebush

has been approved by the Examining Committee for the thesis requirement for the Master of Science degree in Mechanical Engineering at the May 2013 graduation.

Thesis Committee: _____

H.S. Udaykumar, Thesis Supervisor

_____

Albert Ratner

_____

James Buchholz

ACKNOWLEDGMENTS

First and foremost, I would like to thank Uday, Beth, and my parents for their relentless patience and encouragement as I plodded through my work. Without their help and support, this project would not have been possible.

In addition, I would like to thank Eric Osgood and Seth Dillard for never letting me take things too seriously. Graduate school was quite fun for me, and I credit these guys.

TABLE OF CONTENTS

LIST OF TABLES

LIST OF FIGURES

CHAPTER 1

INTRODUCTION AND CURRENT DESIGN CONCEPTS

1.1 Problem Introduction

In December of 2010, a small group of students ventured to India to take part in the first offering of a class taught by Dr. H.S. Udaykumar. The course was designed to investigate the cooking processes of the local Indian villagers outside of Udaipur – a city located in Rajasthan, India (see Figure 1.1). What was found truly surprised the class and instructor. Trees and vegetation had been nearly wiped out, simply because the villagers depended on the firewood to cook their food. Each day, the women and children would go out into the countryside, travelling more than an hour in each direction, in order to gather the necessary wood and brush required to do that day's cooking.

Figure 1.1. Map of Rajasthan

Source: Wikipedia. *Rajasthan.* April 14, 2013. http://en.wikipedia.org/wiki/Rajasthan (accessed April 25, 2013).

Accompanied by a friend of the instructor, Sailesh Rao, the students were also shown a wildlife preserve in which the villagers were not allowed to retrieve materials for cooking and were also not allowed to let their animals graze on the grass. The preserve had previously been a source of firewood and animal grazing. In only a few years, the preserved area had regrown a large amount of its original vegetation; trees had fresh leaves on new branches and the undergrowth had new wild grass.

In Rajasthan, the borders of the region bump up against Pakistan. In the western portion of the state, the Thar Desert is the dominating geographical feature. In recent decades, the borders of the desert have been moving towards the east as vegetation – which provides wind and erosion protection – is removed from the area.

Families are extremely poor yet very conscientious of their lack of resources. For this reason, families in Rajasthan tend to cook indoors so other families cannot see how much or little food they have. Because they cook indoors with firewood, smoke fills the small huts and fills the lungs of the women and children. Across the globe, more than 3 billion people cook and heat their homes with firewood. According to the World Health Organization, nearly 2 million people suffer premature deaths due to illnesses attributable to indoor air pollution every year (World Health Organization 2011).

Conveniently, Rajasthan is located in one of the sunniest areas in India. Solar cooking devices have been designed for use throughout the world, but have failed to catch hold in the areas that need them the most – communities of extreme poverty. Often, these cooking devices will force the participant to cook their food in a manner that breaks with their traditional cooking practices. In some cases, the new cooking devices can be downright unpleasant to use. For example, a design implemented in Rajasthan in 2008 and 2009 reflected the sunlight back towards a cooking surface, though the system was not very accurate. As a result, some of the concentrated sunlight would hit the participants as they were cooking, causing their skin temperature to rise rapidly. Finally, previous solar cookers have required users to cook while the sun is out. In Rajasthan,

though, villagers prefer to cook in the morning and in the evening so that the men can be gone during the day to tend to their other business. New designs for solar cookers need to be easy to use, safe, and be able to blend with the local practices and traditions.

1.2 MEDP Spring 2011

Upon returning to the University of Iowa, Dr. Udaykumar taught the Mechanical Engineering Design Project (MEDP), a class intended to be a capstone project for the senior students. In the class, students were challenged to design and build a solar cooking device that would address the challenges raised by the study abroad group. The final design utilized a parabolic solar collector, sand as an energy storage material, and rice hulls as an insulating material. The parabolic collector was constructed out of polished aluminum and was designed to be aligned in an east-west manner. Rice hulls have excellent thermal properties and are widely available in India for little-to-no cost. Some properties of rice hulls are listed in Table 1.1.

Table 1.1. Thermal properties of rice hulls

Density [kg/m^3]	740
Specific Heat [J/kg*K]	1,098 to 2,754
Thermal Conductivity [W/m*C]	0.0359

Sources: Jha, S., and A. Singh. "Physical and Thermal Properties of Untreated and Chemically Treated Rice Husk." Journal of Agricultural Engineering, 2007: 44.

Juliano, Bienvenido. "Rice: Chemistry and Technology." In Rice: Chemistry and Technology, edited by Bienvenido Juliano, 696. St. Paul, MN: The American Association of Cereal Chemists, 1985.

Upon testing, the original collector did not work as designed. The polished aluminum did not reflect well, the sand's low thermal conductivity restricted the flow of

energy and heat into the storage material, and the device itself weighed well over 500 pounds. Nonetheless, it was a step in the right direction.

1.3 MEDP Fall 2011

The following fall, another senior design class took a stab at some of the design flaws. The majority of the work was intended to improve the thermal conductivity of the storage system. In one particular test, students added aluminum scrap shavings to the sand and with the intent of increasing the thermal conductivity of the sand. In addition, students improved the reflectivity of the parabolic collector by using Mylar to coat the previously-designed collector. The class in the fall was smaller than that from the previous spring, so the students did not attempt to construct a full-scale solar cooking device.

1.4 Second Trip to India

In December of 2011, another group of students, including the author, ventured to India to explore the problem further. Their main intent was to gather data about the cooking patterns and habits of the villagers. Simple thermocouple temperature probes were brought along in order to measure the temperature of the cooking surface. Surveys were created and translated into the local language of the villagers. These surveys were designed to ask questions such as, “How long do you normally cook?” and, “What are some of your complaints with previous cooking systems [designed to replace wood and fire]?” Finally, students measured the dimensions of the traditional cooking setups.

To conduct the surface temperature tests, a K-type thermocouple was attached to a multimeter. The tip of the thermocouple was placed directly onto the tava, or cooking surface, as the villagers were cooking. Once the thermocouple reached steady state, temperatures were read out by the student holding the thermocouple in place and were

recorded by other students in the hut. Cooking surface temperatures ranged from 200 to 250 [C].

When asked about their cooking habits, the villagers said that in general, they cook for about two hours in the morning and two hours in the evening. The average beginning time for the morning meal was sun up, and the average beginning time for the evening meal was sun down. Because they lead such a simple lifestyle, they eat when they're hungry and sleep when they're tired; very little emphasis is placed on doing things at an exact time of day. In addition, there are few clocks for the villagers to read an accurate time.

The complaints of previous systems mainly stemmed from poor integration with prior cultural standards. For example, because the villagers prefer to cook in the morning and in the evening, the solar cooker needs to be able to store enough energy to make it through the night to cook the following morning. Previous designs were not capable of this. In addition, villagers complained that the method of cooking itself was drastically different than what they were used to. Traditionally, the village women cook while sitting on the ground in their huts. The cooking surfaces observed by the students were only 10 to 15 centimeters off the ground. New solar models forced the women to stand up and cook outside, both of which they were uncomfortable doing.

Dimensions of the tavas were recorded between 15 to 25 centimeters in diameter. Most families owned a tava made of clay because they were less expensive than those made of cast iron. Students travelling to India had an opportunity to purchase these tavas while staying in Udaipur. One student purchased a clay tava while another purchased a cast iron tava. Both measured 20 centimeters in diameter.

Students also had the opportunity to visit the headquarters of the Brahma Kumaris in Mount Abu, Rajasthan. At the facility, solar collectors designed by Wolfgang Scheffler were being deployed in order to cook food on a large scale. Scheffler reflectors track the sun and reflect the light so that the resultant rays are roughly horizontal with the ground.

The advantage of the Scheffler is that it allows the user to keep the focal spot stationary throughout the day. In other words, it is capable of tracking the sun's movement. The other advantage of the Scheffler design is that it can be constructed on site using local materials, training, and resources. The Barefoot College, located in Tiloniya, India, regularly constructs Scheffler collectors for the use of solar cooking. Attendees of the college have no formal education and come from all parts of the globe. Scheffler collectors are able to be constructed for a cost of approximately $250.

1.5 MEDP Spring 2012

In the spring semester of 2012, another small group of students worked on the solar cooking device as part of their senior design project. The main goal of the students was to build a Scheffler collector. Using free instructions provided on Wolfgang Scheffler's website (Scheffler 2013), students successfully built a 2.5 meter collector.

1.6 Collector Types

There were three main types of solar collectors for consideration: Parabolic, Scheffler, and Fresnel. Other types of solar collectors are certainly available on the market, but few other formats have been put into place for the use of solar cooking.

Parabolic collectors take advantage of the fact that parabolas have a common focal point. Figure 1.2 displays this feature.

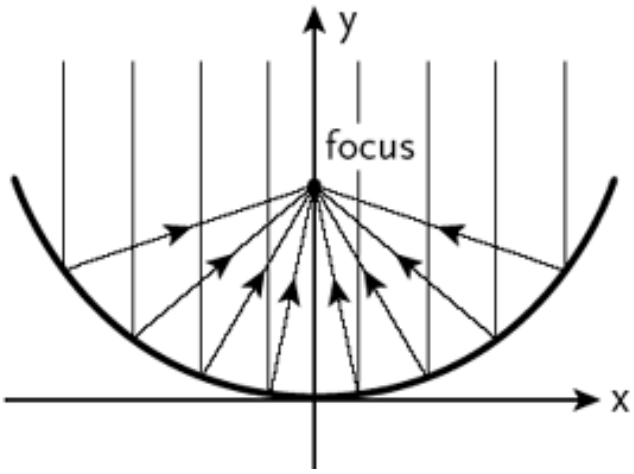

Figure 1.2. Focal properties of parabolas

Source: PBS. Finding the Focal Point. 2013. http://www.pbs.org/wgbh/nova/education/activities/3406_solar_03.html (accessed March 27, 2013).

Linear parabolic collectors are set up in such a way that the focal point actually becomes a focal line. Parabolic dishes are set up the same way a satellite dish for a TV focuses the signal to one point.

Wolfgang Scheffler took the concept of a parabolic collector that focuses the sun's energy to a point and combined it with solar tracking. If the focal point of the collector is far enough away from the parabola, then with the proper setup, the focal point can actually be indoors. Thus, with the Scheffler collector, there are unique possibilities for better cultural integration to allow the cooking surface to be inside. His system uses an ingenious counterweight design as the energy required to move the collector throughout the day. A 35 kilogram block of stone is lifted approximately 20 centimeters at the beginning of the day, then a system of gears slowly lowers the weight as the reflector rotates, much like how a clock will rotate its hands as the spring tension is slowly released.

Fresnel lenses allow the sun to pass through a glass or plastic interface, and the lenses are able to achieve extremely high concentration ratios. In order to work throughout the day, though, the Fresnel lens would need to be placed on a tracking device. Current designs utilizing Fresnel lenses require the sun to be up in order for the solar devices to work.

1.7 Storage Types

There were two formats of energy storage considered for the solar cooking device. Sensible storage is simply the storage of energy within an object due to a temperature difference. The amount of energy in Joules can be calculated by considering the thermal heat capacity, mass, and difference in temperature: The change in energy is simply the mass in kilograms, multiplied by the heat capacity (units of joules per kilogram kelvin) and the difference in temperature as measured in kelvin. The resulting change of energy will have units of joules.

Latent energy storage uses a phase change – solid to liquid, for example – to add additional capacity for storage. The latent heat of melting for water is 334,000 [J/kg]. If the right material is selected that has a melting temperature that is close to the ideal cooking temperature, then the cooking can take place at or near the preferred cooking temperature as the storage material transitions from liquid to solid.

1.8 Solar Data for Rajasthan

As was mentioned previously, Rajasthan is one of the sunniest regions in all of India. The Department of Science and Technology within the Government of India commissioned a report entitled, *Solar Radiation Over India*. Within the report, specific data are given for many cities within India, including Udaipur. Table 1.2 shows the direct daily radiation on a horizontal surface for Udaipur. Although Udaipur is in the Northern Hemisphere and one would expect an increase in the daily radiation during the months of

June, July, August, and September, the monsoon season makes solar energy hard to come by. Nonetheless, the remaining eight months of the year have plenty of clear skies. (Mani and Rangarajan 1982)

Table 1.2 Direct daily radiation on a horizontal surface in Udiapur

Month	**Direct Daily Radiation [kWh/m^2]**
January	3.908
February	4.707
March	4.937
April	5.357
May	5.523
June	3.956
July	1.880
August	1.878
September	3.215
October	4.596
November	4.453
December	3.687

Source: Mani, Anna, and S. Rangarajan. Solar Radiation over India. Book, New Delhi: Allied Publishers Private Limited, 1982.

1.9 Conclusion

After the past few years, a few key elements of a successful design have surfaced. First and foremost, the cooking device must be able to store energy overnight and throughout the day. Without a storage system, the villagers are forced to cook during the day while the sun is up. The cooking surface must be between 15 and 25 centimeters in

diameter, preferably at 20 centimeters. The cooking device must provide heat for two hours each morning and each evening. Finally, the surface temperature of the cooking surface needs to be maintained at between 200 and 250 Celsius. For the purposes of this project, solar collector designs were largely passed over. There were a number of options available that, with a little tweaking, would likely be able to work. The main thrust of this project was targeted at the storage system, as that was the main obstacle to overcome.

CHAPTER 2

EXPERIMENTAL METHODOLOGY

2.1 Cooking Surface Test

After the author returned from India in the spring of 2012, the required cooking surface temperature was known to be between 200 and 250 Celsius. The next necessary step was to design an experiment that would reveal the required power in order to achieve these temperatures.

To do so, a box measuring 30 centimeters in width, 30 centimeters in depth, and 20 centimeters in height was used. The box was made of wood measuring 1 centimeter in thickness. The top of the box was left open, thus leaving the box with five sides of wood and one with no cover. The box was stuffed with common household insulation in order to limit heat transfer to the sides and to the base. A circular heating element was placed on top of the insulation. A 20 centimeter diameter cast iron tava was placed on top of the heating element. The heating element was plugged in to a variable AC controller, which provided different amounts of AC current into the heating element. The variable AC controller was plugged into a wattmeter, which allowed the user to keep track of the power being provided to the system. Figure 2.1 shows the basic experimental setup. Finally, a thermocouple and micrometer were used to record the temperatures at the center the cooking surface. To conduct the test, the variable AC controller was set at a certain percentage, the system was allowed to reach a steady state temperature, the wattage was read from the wattmeter, and the corresponding temperature was recorded. The setup regularly took 30 minutes or more to reach its steady state temperature.

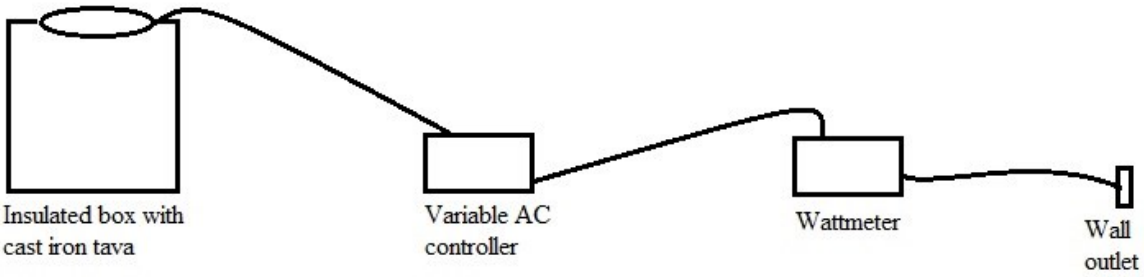

Figure 2.1. Experimental test diagram

CHAPTER 3
EXPERIMENTAL RESULTS

3.1 Cooking Surface Test

After performing the test, data were organized into Table 3.1 and Figure 3.1, located at the end of the chapter.

The results of the test show that in order to maintain a cooking temperature between 200 and 250 [C], as is preferred in the villages, an input power of 193 to 263 watts is required. Granted, the test has some obvious limitations. Most notably, the insulation provided by the box and household fiberglass is nowhere near as good as the mud and dirt in the huts. The fires inside the huts are totally surrounded by a mud fire pit. When students were performing the tests with the multimeter, the ground beneath their feet was a very reasonable and touchable temperature. In estimation, it was thought to be only slightly warmer than room temperature, or approximately 35 [C]. The box in the experiment, however, reached temperatures of over 60 [C]. With four exposed sides, each radiating and convecting at such a warm temperature, there were bound to be plenty of losses. When considering a construction plan in future chapters, aluminum is the material of choice for the cooking surface. The emissivity of aluminum is lower than that of cast iron, thus at the same temperature, aluminum would emit less energy via radiation than cast iron. With less energy being lost due to radiation, aluminum is a more efficient choice than cast iron.

Table 3.1. Cooking surface test results

Percent	Watts	Temperature [C]
0	0	27
4	6.4	34
8	14.8	43
12	27.7	55
16	44.7	75
20	65.9	94
24	87.1	114
28	120	142
32	145	167
34	148	168
35	152	170
36	165	180
37	170	185
38	180	191
39	188	198
40	193	203
41	207	210
42	215	216
43	226	227
44	234	232
45	241	236
46	252	240
47	263	246

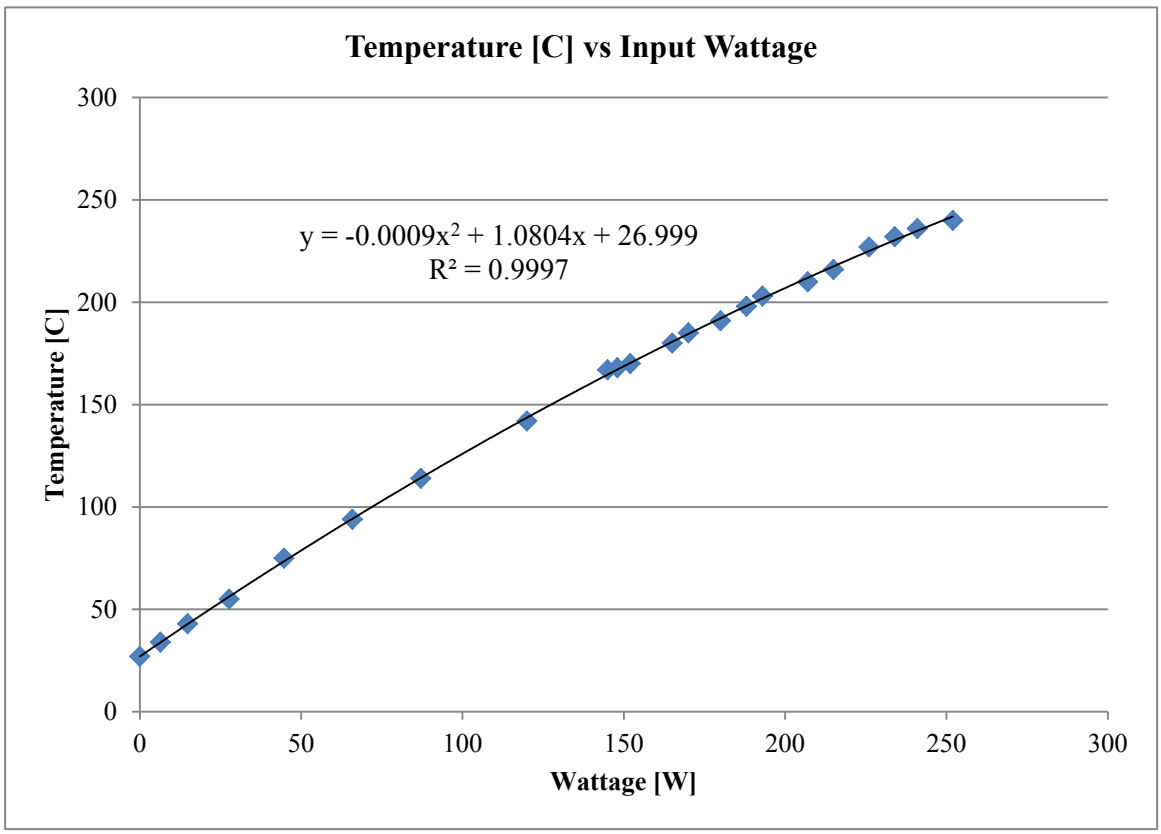

Figure 3.1 Cooking surface test results

CHAPTER 4

SIMULATION METHODOLOGY

4.1 Simulation Goals

Because constructing new designs of the solar cooking device takes both time and money, the preferred method to design a solar cooking device was to use computer simulations. Ultimately, the end goal was to offer energy storage solutions for a solar cooking device. Unfortunately, this project did not get as far as constructing physical cooking devices based on the simulations.

In addition to coming up with options for energy storage, one additional goal for the simulations was to present an optimized energy delivery design. This design would need to be better at delivering the energy in an efficient manner such that it maintains a more constant cooking temperature over the course of the two hours.

4.2 Simulating Heat Transfer

ANSYS Fluent is a program that allows people to simulate Computational Fluid Dynamics, or CFD. This is a computer-based modeling approach that can either be run on a single local machine, or on a cluster of thousands of computers.

There are three basic forms of heat transfer: conduction, convection, and radiation. For the forms of heat transfer involving direct contact between two bodies, Fluent uses the basic laws of conduction to do its modeling. The basic governing equation is called the heat diffusion equation, and is listed as Equation (1). This particular version of the heat diffusion equation uses cylindrical coordinates, given the cylindrical nature of the cooking surface, and thus energy storage requirements. True, the storage itself need not be cylindrical or radial in shape, but a cylindrical approach offers the most efficient manner in which to store the energy based on a given volume.

$$\frac{1}{r}\frac{\partial}{\partial r}\left(kr\frac{\partial T}{\partial r}\right)+\frac{1}{r^2}\frac{\partial}{\partial \phi}\left(k\frac{\partial T}{\partial \phi}\right)+\frac{\partial}{\partial z}\left(k\frac{\partial T}{\partial z}\right)+\dot{q}=pc_p\frac{\partial T}{\partial t} \quad (1)$$

Convection can be modeled in Fluent in multiple ways. One of the most complicated models would be to simulate the eddies and convection currents that would be found in the air just above the cooking surface. Unfortunately, this style of simulation requires significant computing power – power not readily available to the author. Instead, Fluent also allows the user to input a heat transfer coefficient, *h*, for the surrounding fluid. The air inside the hut was not quite static, but it was certainly not breezy, either. Thus, a heat transfer coefficient of 20 [W/m^2*K] was selected because it was in the overlapping area of values for free convection and forced convection for air.

Finally, modeling radiation in Fluent also has many options. The user can make a very complicated setup, designed to model the radiation transfer very accurately. Or, the radiation setup can be very simple – only requiring the input of the surrounding temperature and emissivity. For the sake of minimizing computing requirements, the latter option was selected. The surrounding temperature was assumed to be constant for the sake of simplicity, and was assumed to be 297.46 [K], which was the average air temperature for Udaipur computed by the team who wrote *Solar Radiation over India* (Mani and Rangarajan 1982). The proposed cooking surface was made of aluminum, and the rice hulls were encased in a wood structure. Aluminum and wood have emissivity values of 0.15 and 0.85, respectively (Engineering Toolbox 2012).

4.3 Simulation Setup

The basic concept for the design of the solar cooking device originated from the notion of using a 50 kilogram cylinder of aluminum as the storage material. Optimized for height and radius, the cylinder would stand 18 centimeters tall and have a radius of 18 centimeters. This size was kept constant throughout all of the simulations, so it should be immediately noted that more variations of height and radius should be tested in the future

to present a more complete body of work. The insulating material, rice hulls, was originally a plain cylinder. The drawbacks of such a system became evident, though, when much of the heat loss was near the base of the system. Thus, a wider base was required, and a more conical shape of the rice insulation emerged. For most of the simulations, Lithium Nitrate is used as a storage material. Thermal properties of Lithium Nitrate are listed in Table 4.1.

Table 4.1. Thermal properties of Lithium Nitrate

Density [kg/m^3]	2,380
Specific Heat, Solid [J/kg*K]	0.585 + 2.182E-3*T[K]
Specific Heat, Liquid [J/kg*K]	1.681 + 6.389E-4*T[K]
Latent Heat of Melting [J/kg]	357,000
Solidus Temperature [K]	500
Liquidus Temperature [K]	540
Thermal Conductivity [W/m*K]	0.511
Viscosity [kg/m*s]	1.95

Source: Kenisarin, Murat M. "High-temperature phase change materials for thermal energy storage." Renewable and Sustainable Energy Reviews, 2009: 955-970.

The simulations in Fluent were computed by using a transient 2D-axisymmetric model. The Energy and Solidification & Melting equations were turned on. Material properties were modified to add Lithium Nitrate and rice hulls. The cell zone conditions were then appropriately changed to reflect their appropriate materials. For example, the PCM (phase change material) zone condition was altered so that it utilized Lithium Nitrate instead of air as the fluid of choice. Boundary conditions at the base of the model for both aluminum and rice were set as adiabatic, or having no heat transfer between the

base and the ground. Boundary conditions at the outside of the rice hulls were set to reflect the radiation and convection terms previously described. Finally, boundary conditions for the cooking surface were set depending on the time of day. The cooking times and length were determined by the surveys conducted with the villagers. The energy input period, from 9:00am to 4:30pm, was designed to transfer 5 [kW-h] into the storage device over the course of seven and a half hours. Table 4.2 describes the boundary conditions.

Table 4.2. Cooking surface boundary conditions

Time	**Boundary Condition**
12:00am – 7:00am	Mixed (radiation and convection)
7:00am – 9:00am	If the cooking surface temperature was higher than 225 [C], the boundary condition was set to a heat flux designed to draw 250 [W] from the surface. If the cooking surface temperature was lower than 225 [C], the boundary condition was left at mixed.
9:00am – 4:30pm	A heat flux boundary condition was specified such that the total heat transfer into the system over the course of the day was 5 [kW-h]. The input fluctuated like a basic sinusoidal wave – at 9:00am and 4:30pm, the input was zero; at 12:45pm the input reached its daily maximum.
4:30pm – 7:00pm	Mixed (radiation and convection)
7:00pm – 9:00pm	Same as 7:00am – 9:00am
9:00pm – 12:00am	Mixed (radiation and convection)

It should be immediately noted that the settings of Fluent did not allow for a simultaneous heat flux *and* mixed boundary condition. Thus, while the cooking surface was being heated to add energy, it was *not* also losing energy due to convection and radiation. The only energy dispersal mechanism was to conduct the energy into the storage material.

The solution method was the SIMPLE method, using first order upwind momentum and second order upwind energy methods. The solution was initialized at 297.46 [K]. Calculations were performed to simulate time steps of 30 seconds, and data were recorded every 20 times steps, or every 10 minutes of simulated time.

CHAPTER 5

SIMULATION RESULTS

5.1 Pure Conduction

The first test performed was with aluminum. The basic layout of the design is shown in Figure 5.1, and the corresponding mesh is shown in Figure 5.2. The material with the square shape is the aluminum, while the material with the trapezoidal shape is the rice husk insulation. It should be noted that for this and all subsequent layout and mesh figures, the figure is simply a 2D slice of the layout beginning at a radius of zero. The real design of the model would be cylindrical for the aluminum or energy storage unit, and slightly conical for the insulation.

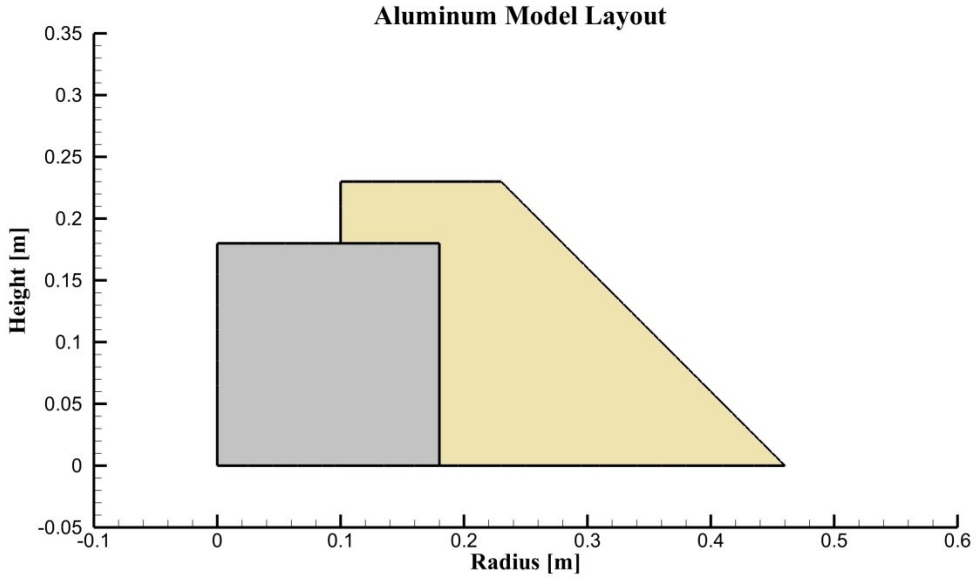

Figure 5.1. Aluminum Model Layout

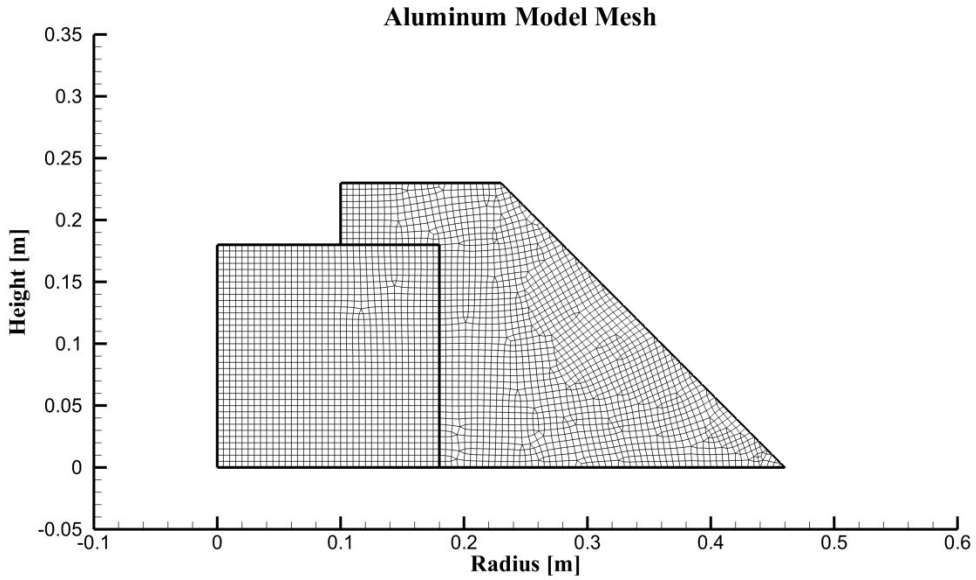

Figure 5.2. Aluminum Model Mesh

The mesh, created in ICEM CFD, was specified to have a minimum density of 0.005 meters between grid points. This mesh density holds true for all subsequent simulations.

Figures 5.3 and 5.4 show the temperature recorded at 0.5 cm below the cooking surface and 0.5 cm above the base, respectively. The first thing to notice is that due to the extremely high value of thermal conductivity in aluminum, the surface and base temperatures are nearly identical. The main issue with aluminum is that the material is too hot or too cold when it is time to cook. At 7pm, the surface temperatures are 400 [C] or more, which is totally unreasonable to cook. At 7am, the surface temperatures are closer to 200 [C], which is too low of a starting temperature. Something else is needed that will allow for plenty of energy to be stored without cooking at such a ridiculous temperature.

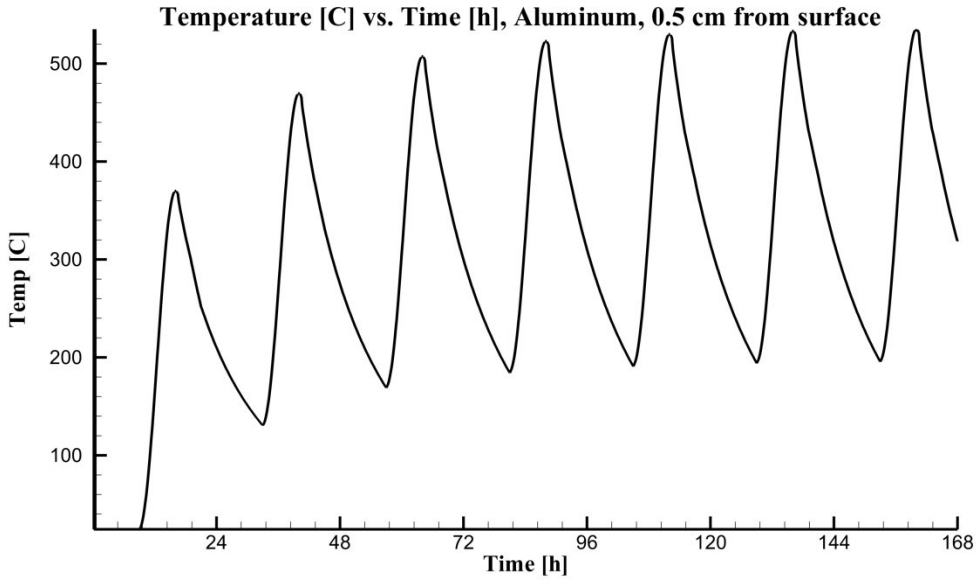

Figure 5.3. Aluminum Surface Temperature

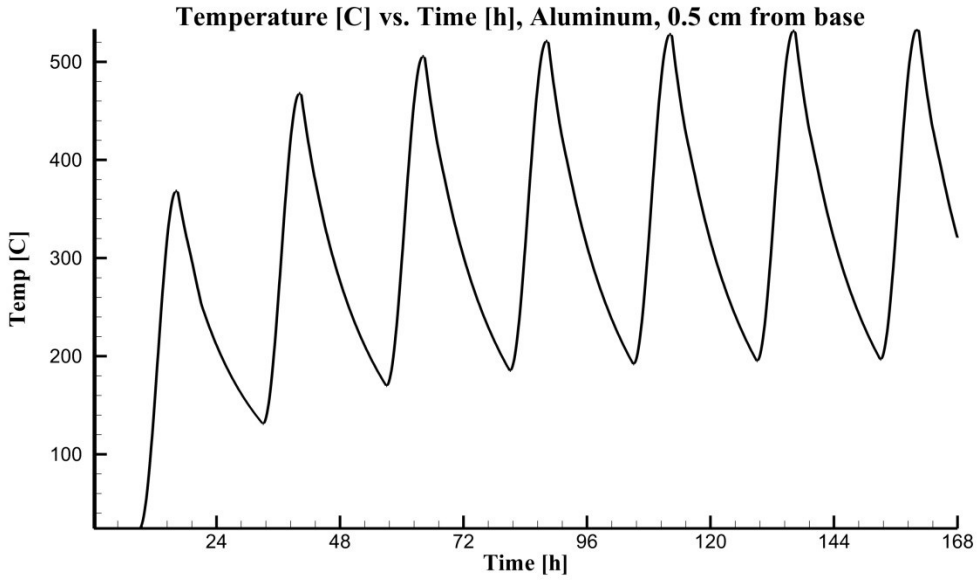

Figure 5.4. Aluminum Base Temperature

5.2 Phase Change

The next test performed was with standard Lithium Nitrate. Due to the liquidus nature of the material, an aluminum casing would be necessary to contain the material, thus it is included as a shell around the Lithium Nitrate. Figures 5.5 and 5.6 show the layout and mesh, respectively.

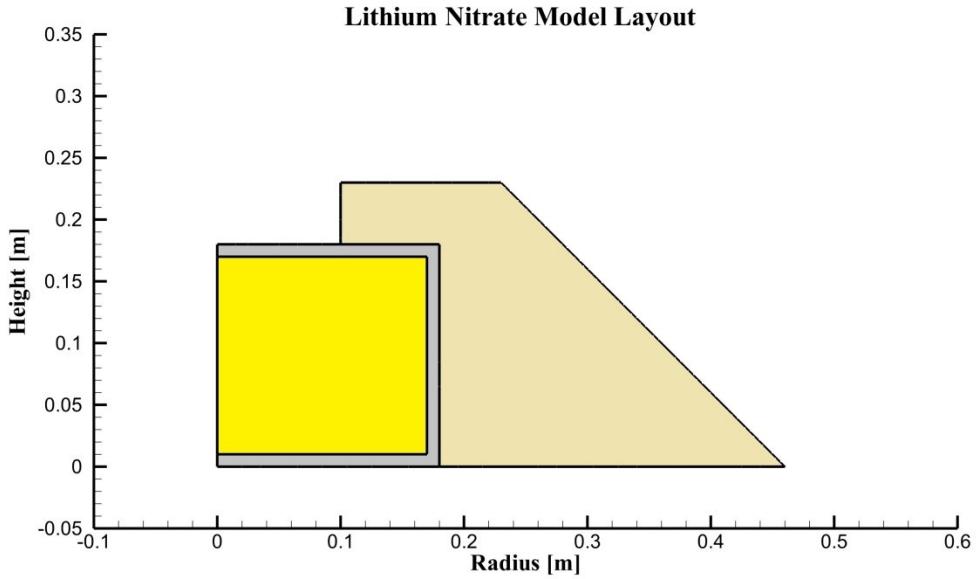

Figure 5.5. Lithium Nitrate Model Layout

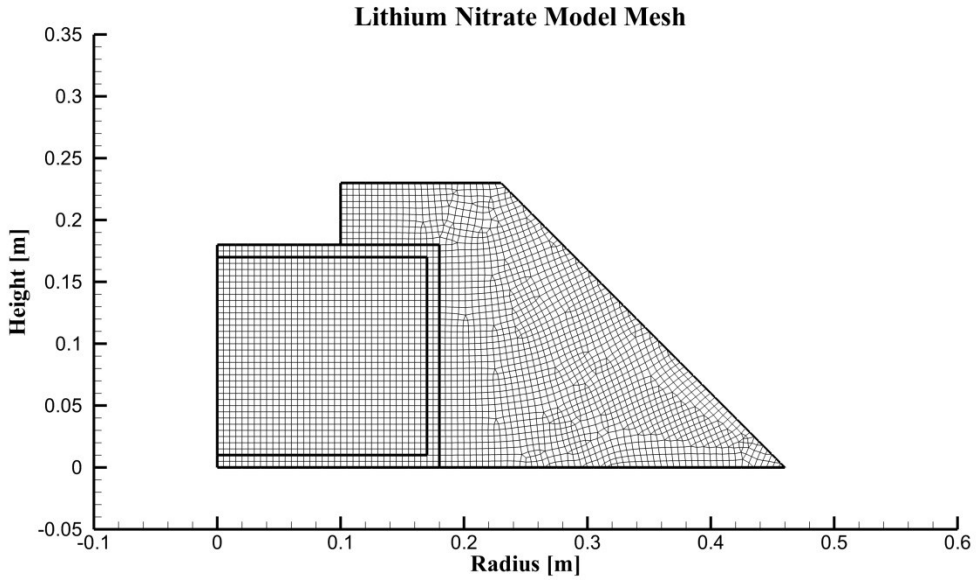

Figure 5.6. Lithium Nitrate Model Mesh

Figures 5.7 and 5.8 show the surface and base temperatures, respectively. The Lithium Nitrate has very poor conduction characteristics. Rather than the thermal conductivity of aluminum, which is over 200 [W/m*K], the thermal conductivity of the Lithium Nitrate is 0.511 [W/m*K]. For this reason, the heat near the edges of the aluminum was not able to disperse very quickly and temperatures became locally very hot – well over 800 [C]. The nice thing about the Lithium Nitrate is that during the 2.5 hour resting period from 4:30pm to 7:00pm, the temperatures dropped 400 [C] to cook at 402 [C], which is slightly more manageable. The main drawback about this design, though, is that the temperatures never remained over 225 [C] in the morning, which was the cutoff for beginning a cooking session.

The simulations did not consider the possibility of natural convection within the Lithium Nitrate. The natural convection would have aided in the dispersal of energy. Because of this, it would have also led to a more even temperature distribution. It should be considered for future simulations.

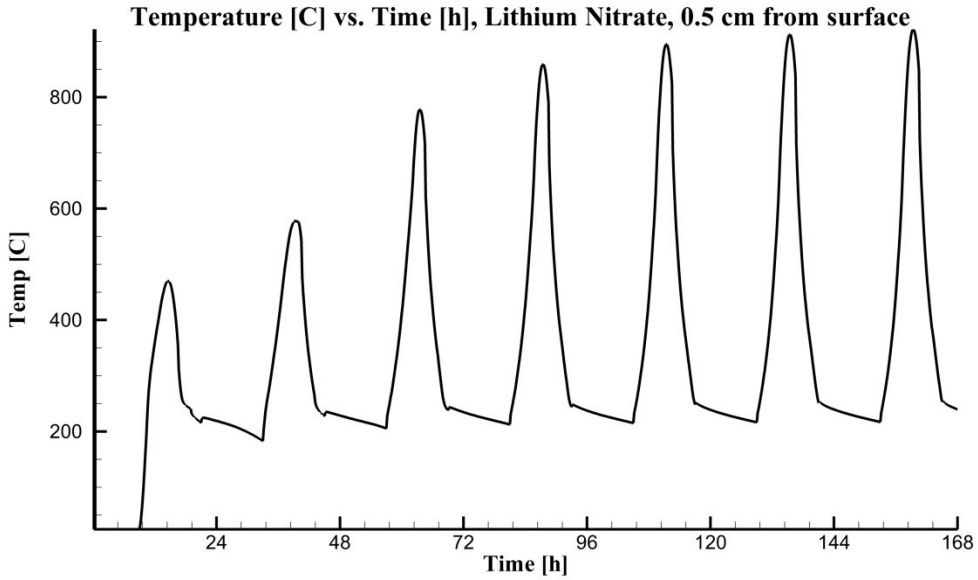

Figure 5.7. Lithium Nitrate Surface Temperature

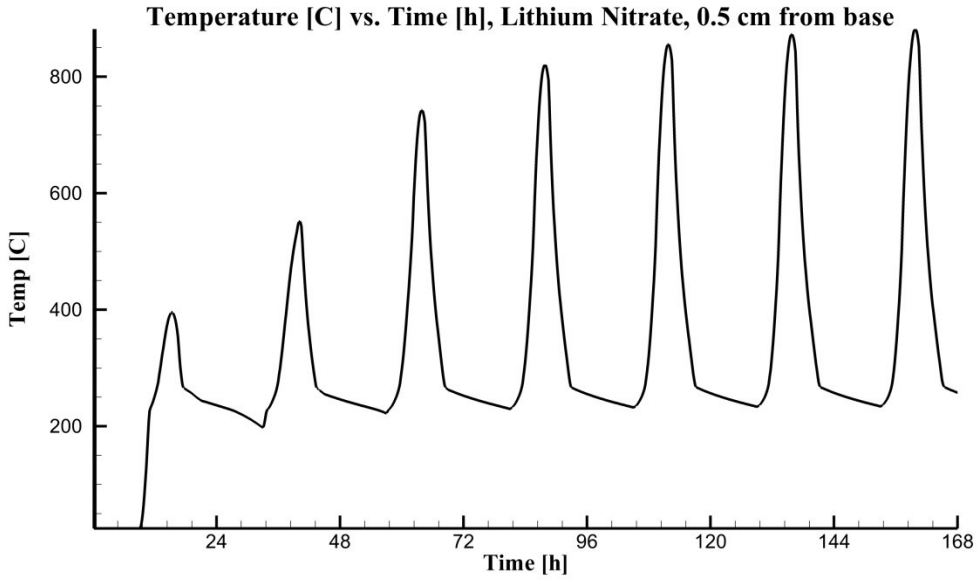

Figure 5.8 Lithium Nitrate Base Temperature

Another Lithium Nitrate model was considered in which the thermal conductivity was artificially raised by a factor of ten from 0.511 [W/m*K] to 5.11 [W/m*K]. This rise could represent doping the Lithium Nitrate with aluminum scrap shards, for example. The layout and mesh are included in Figures 5.9 and 5.10, respectively.

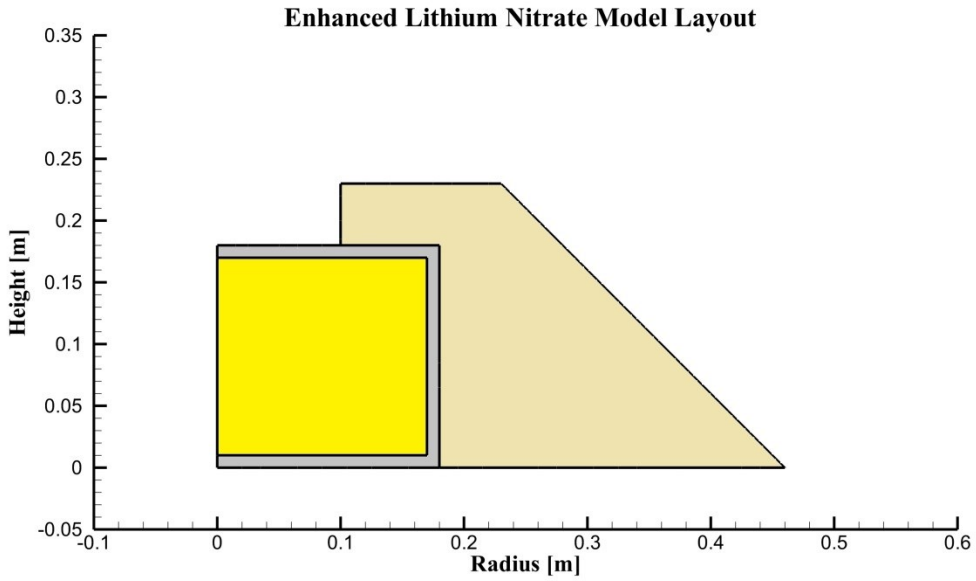

Figure 5.9. Enhanced Lithium Nitrate Model Layout

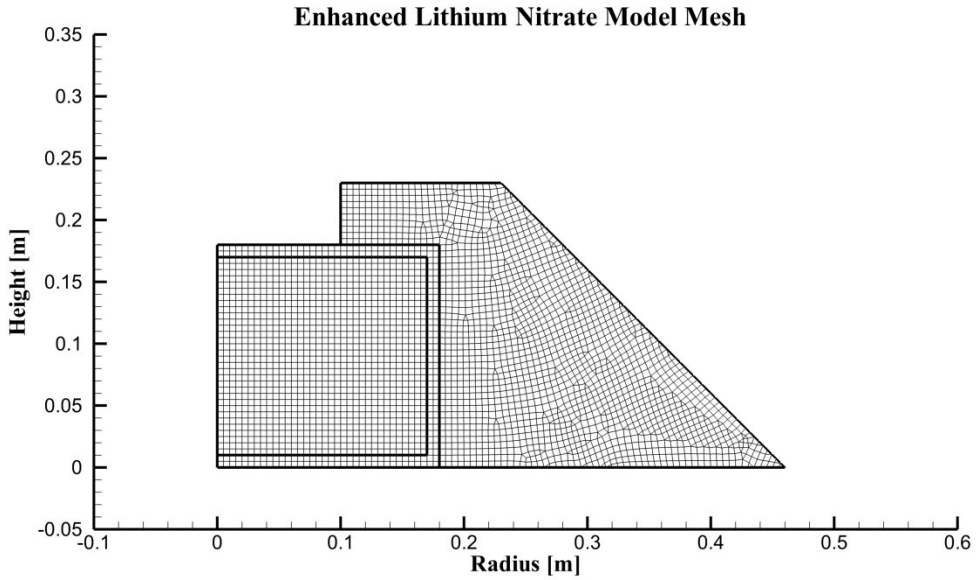

Figure 5.10. Enhanced Lithium Nitrate Model Mesh

One will notice that the mesh and layout are identical to that of the standard Lithium Nitrate case.

Figures 5.11 and 5.12 show the surface and base temperatures, respectively. After the second day of heating, the enhanced model was warm enough to cook in the morning. This signifies that due to the higher thermal conductivity, the energy was able to penetrate into the Lithium Nitrate. There appear to be two phases to the energy input periods. First, the temperature rises to approximately 390 [C], then the temperature spikes for the remainder of the heating session. This is due to the fact that the Lithium Nitrate immediately surrounding the cooking surface have been cooled below the solidus temperature. Thus, during the first phase, energy is being put into the system, but there is not an immediate return in temperature increase. During the second phase, once the material has reached the liquidus temperature, the remaining energy input is directly translated into an increase in temperature. The main drawback of the system is that it took

5 days to reach a steady state. With a day of clouds, the Lithium Nitrate models would not be able to retain their energy.

There are several features of the graphs that are represented in many of the other graphs throughout this chapter. First is the two-phase temperature increase as previously discussed. Second is the rather abrupt stabilization of temperature around 267 [C]. This corresponds to the beginning of the transition between liquid Lithium Nitrate and solid Lithium Nitrate. Finally, the drop in temperature that appears just before the heating sessions is caused by the morning cooking sessions. Neither the aluminum nor standard lithium nitrate models were at an appropriate temperature to cook in the morning, so neither model exhibits this characteristic.

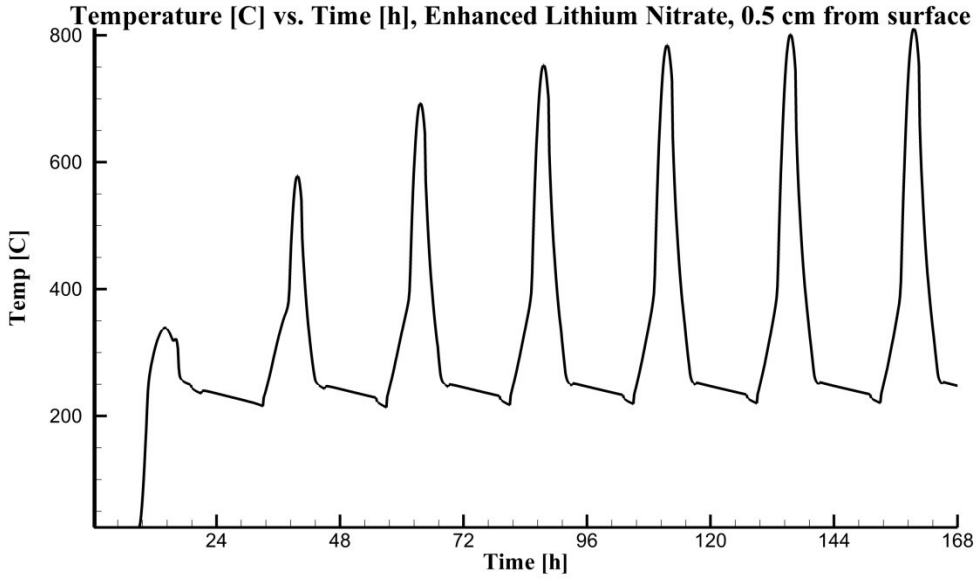

Figure 5.11. Enhanced Lithium Nitrate Surface Temperature

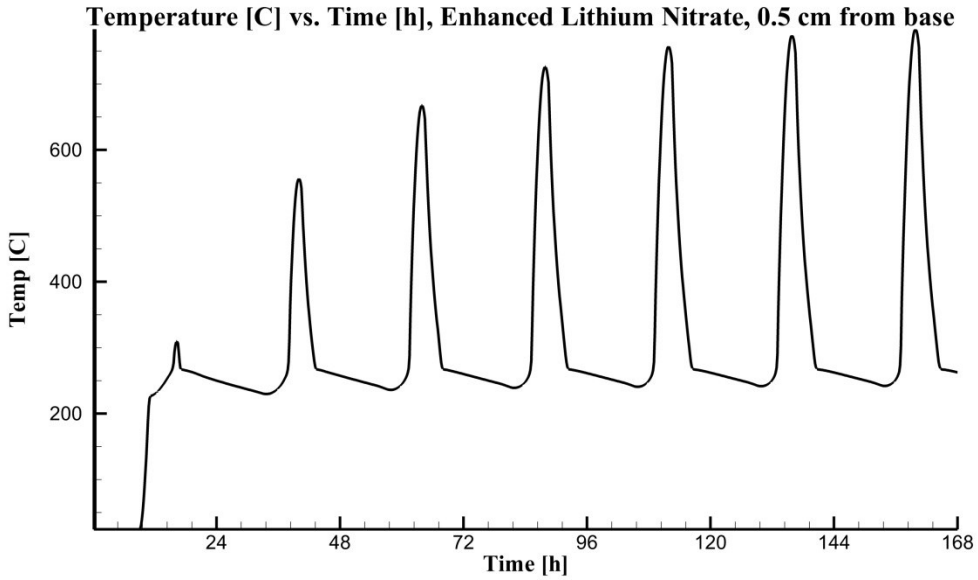

Figure 5.12. Enhanced Lithium Nitrate Base Temperature

5.3 Mixed Phase Change and Conduction

A strictly aluminum or strictly Lithium Nitrate solution is not the ideal case. Instead, different combinations of both Lithium Nitrate and aluminum were tried. The first two combinations use horizontal and vertical aluminum fins extending into the Lithium Nitrate. Figures 5.13, 5.14, 5.15, and 5.16 show the horizontal fins layout, horizontal fins mesh, vertical fins layout, and vertical fins mesh, respectively. The fins are two centimeters in thickness and leave four centimeters of Lithium Nitrate between pieces of aluminum.

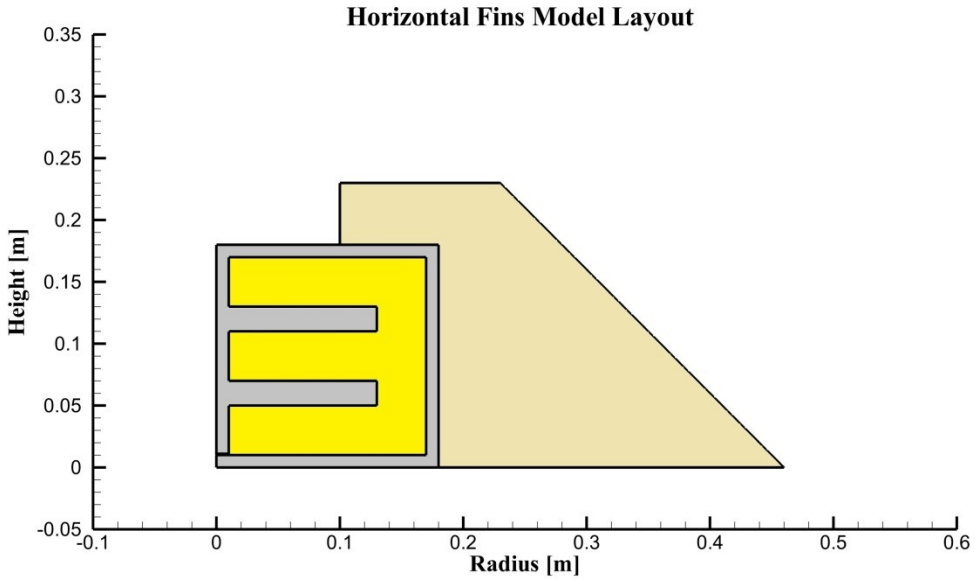

Figure 5.13. Horizontal Fins Model Layout

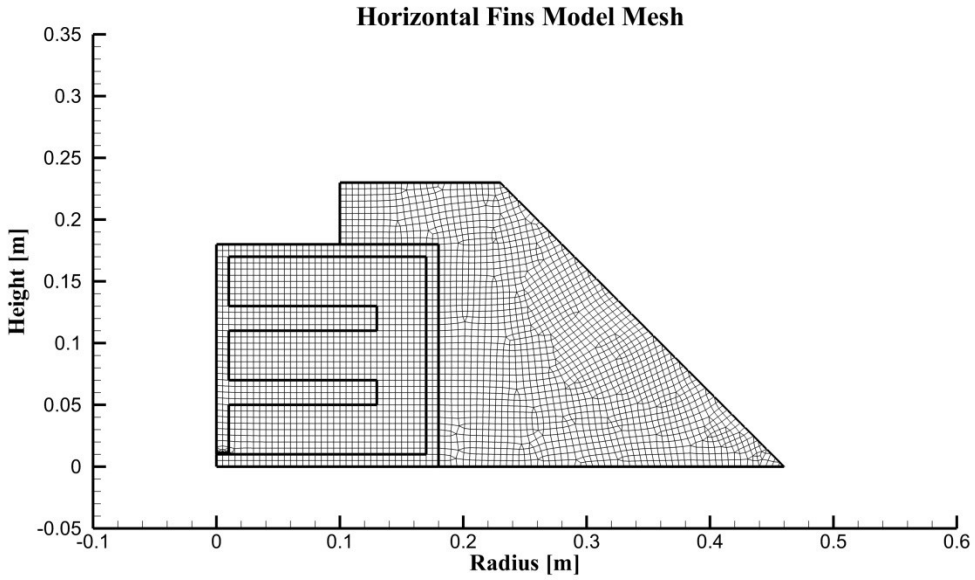

Figure 5.14. Horizontal Fins Model Mesh

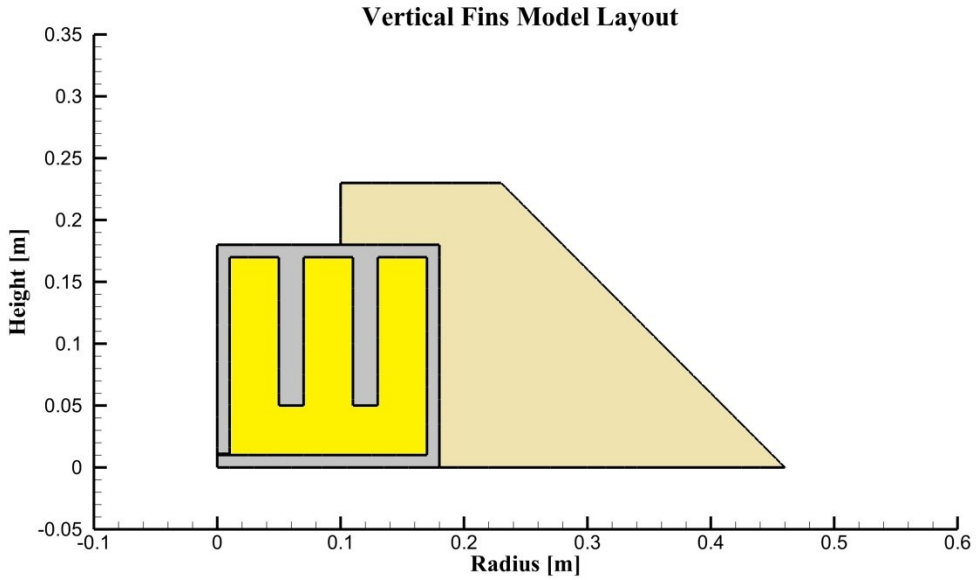

Figure 5.15. Vertical Fins Model Layout

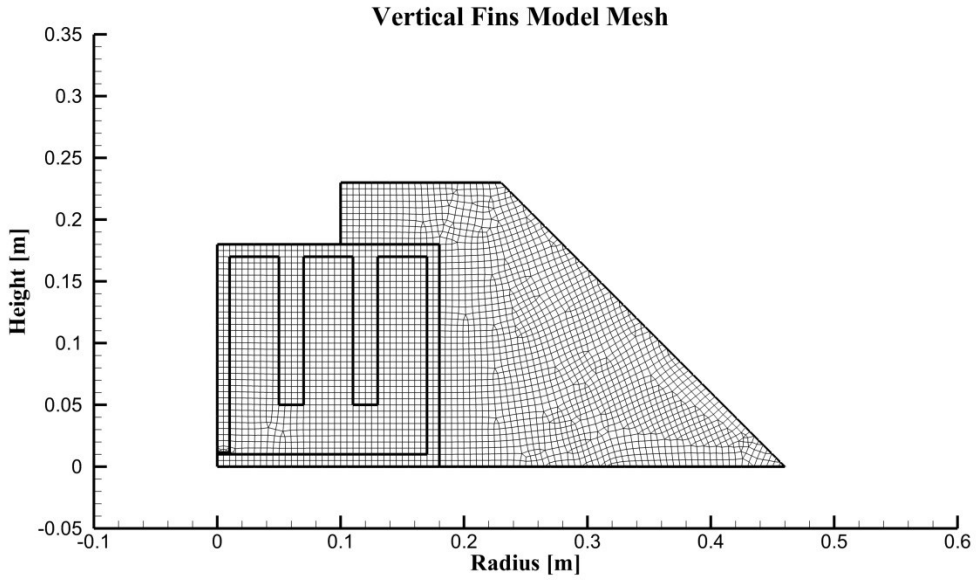

Figure 5.16. Vertical Fins Model Mesh

Figures 5.17, 5.18, 5.19, and 5.20 show the horizontal fins surface and base temperatures, and the vertical fins surface and base temperatures, respectively.

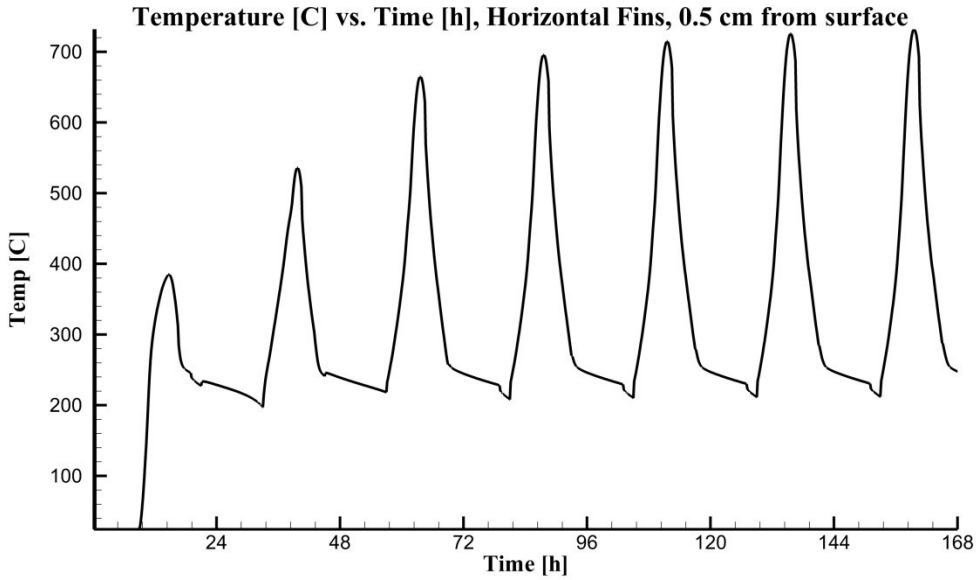

Figure 5.17. Horizontal Fins Surface Temperature

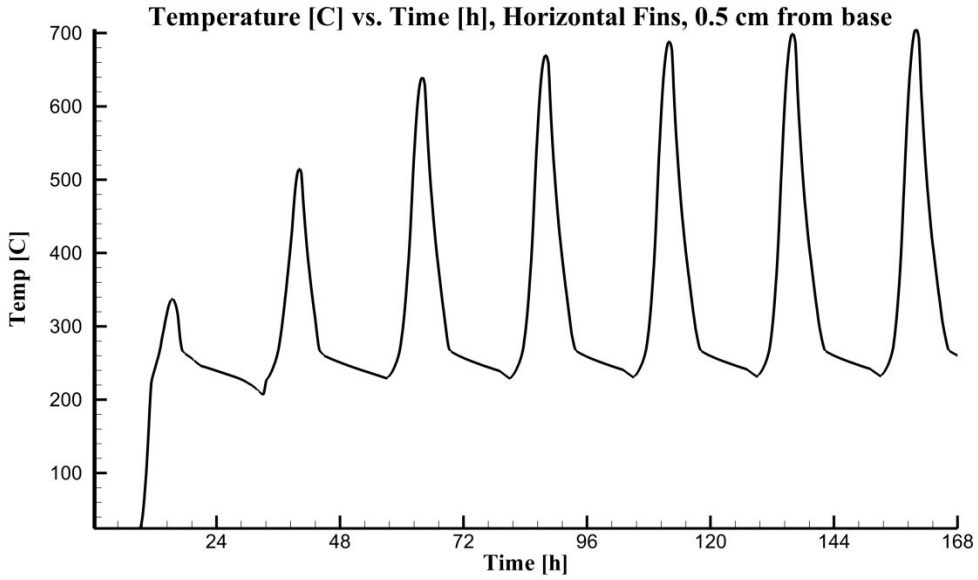

Figure 5.18. Horizontal Fins Base Temperature

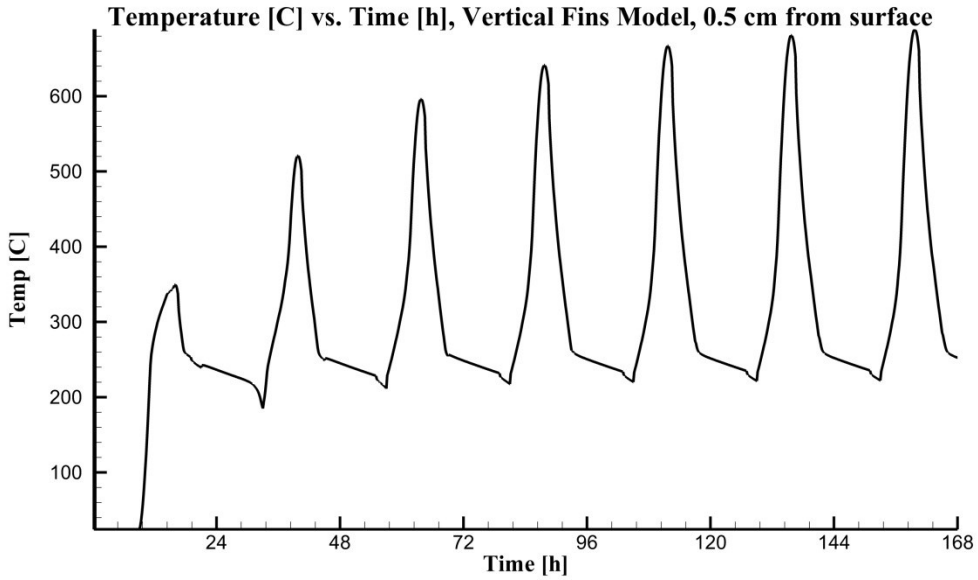

Figure 5.19. Vertical Fins Surface Temperature

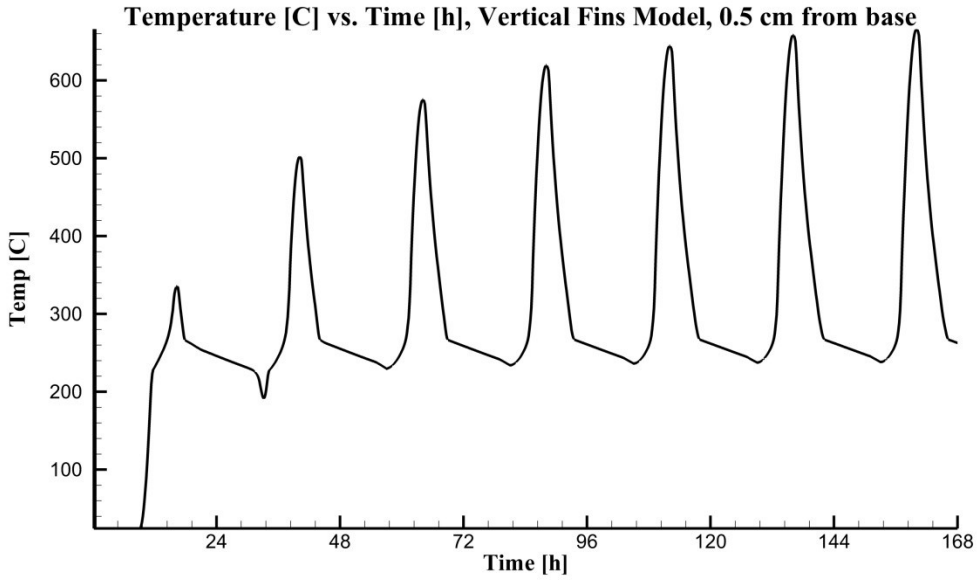

Figure 5.20. Vertical Fins Base Temperature

The main difference between horizontal and vertical models is that the vertical fin model has a lower cooking temperature in the evening. In this case, that is a good thing,

as it brings the cooking temperature to closer to the desired temperature. In addition, the vertical fins model reached a peak temperature of approximately 680 [C], whereas the horizontal fins model reached a peak temperature of approximately 720 [C]. In the relative scheme of things, both are outrageously hot. It is important to keep in mind, though, that the simulation does not allow for any cooling out of the cooking surface as it is being warmed. In addition, the simulations did not account for natural convection. Had it been considered, natural convection would have aided the vertical fins model more than the horizontal fins model by allowing the convecting eddies to travel farther as they rise, thus affecting a greater volume of material.

The next simulation was geared at determining whether it would be beneficial to raise the thermal conductivity of the Lithium Nitrate with the vertical fins model. Just like earlier, the thermal conductivity was artificially raised by a factor of ten. Figures 5.21, 5.22, 5.23, and 5.24 show the model layout, mesh, surface temperature, and base temperature, respectively, for the enhanced Lithium Nitrate with vertical fins model.

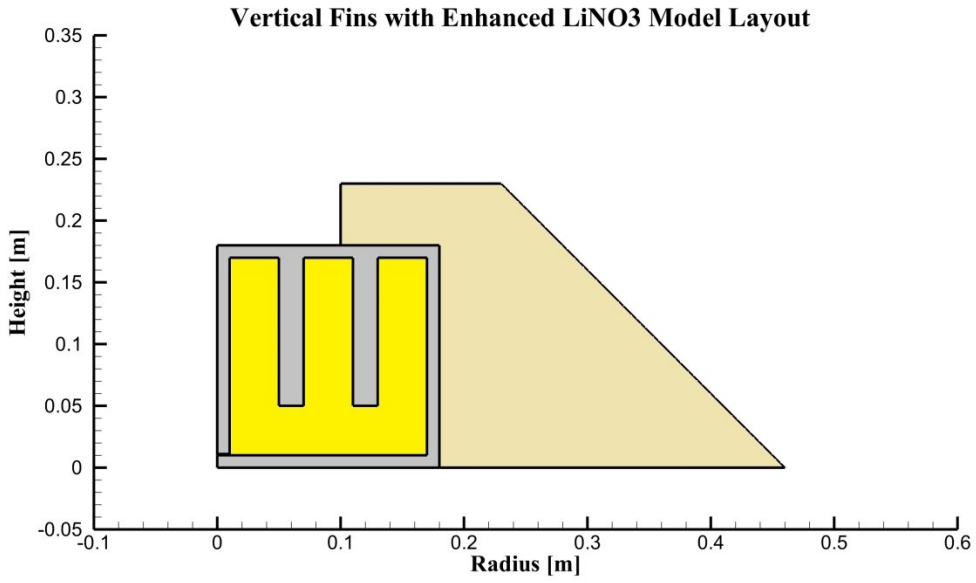

Figure 5.21. Vertical Fins with Enhanced LiNO3 Model Layout

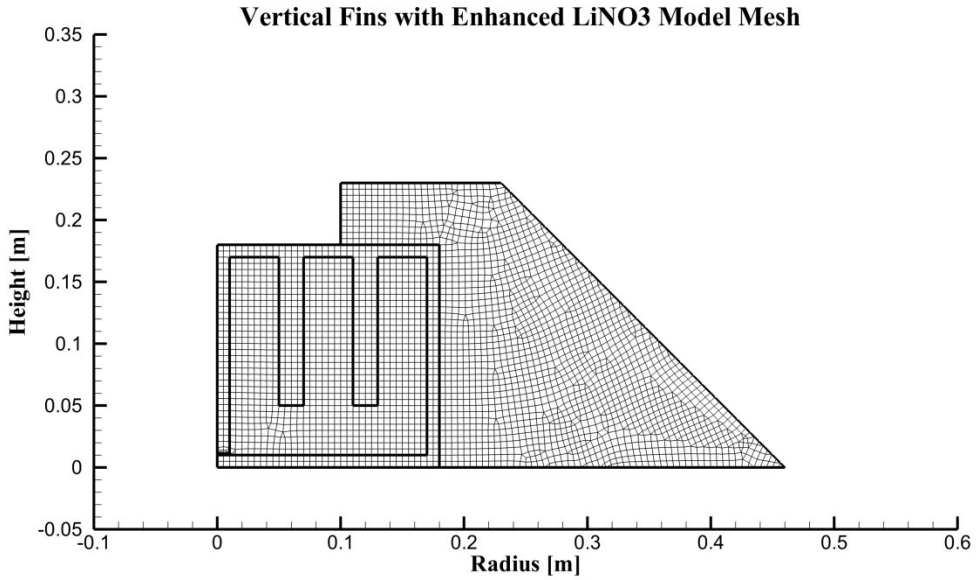

Figure 5.22. Vertical Fins with Enhanced LiNO3 Model Layout

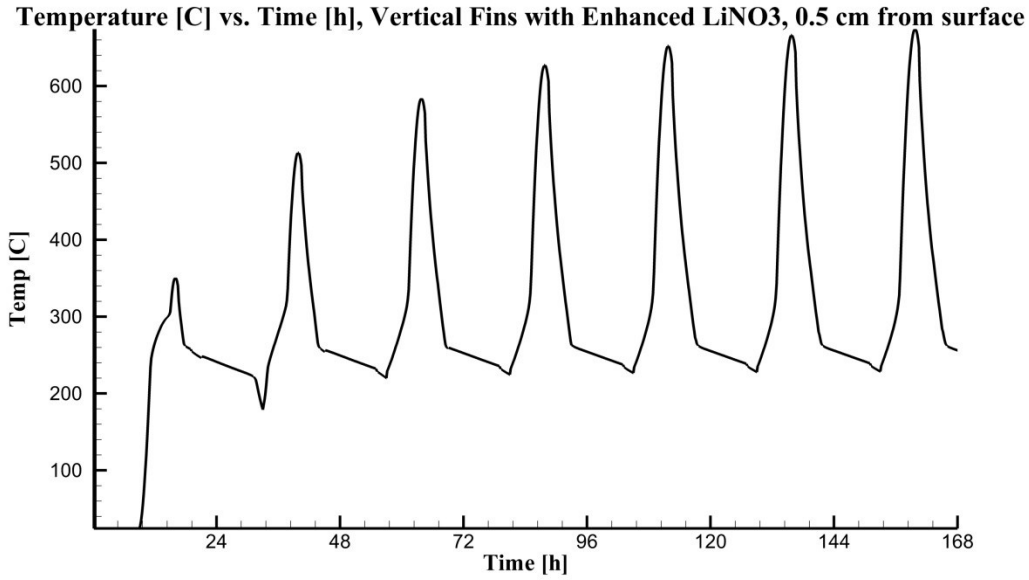

Figure 5.23. Vertical Fins with Enhanced LiNO3 Surface Temperature

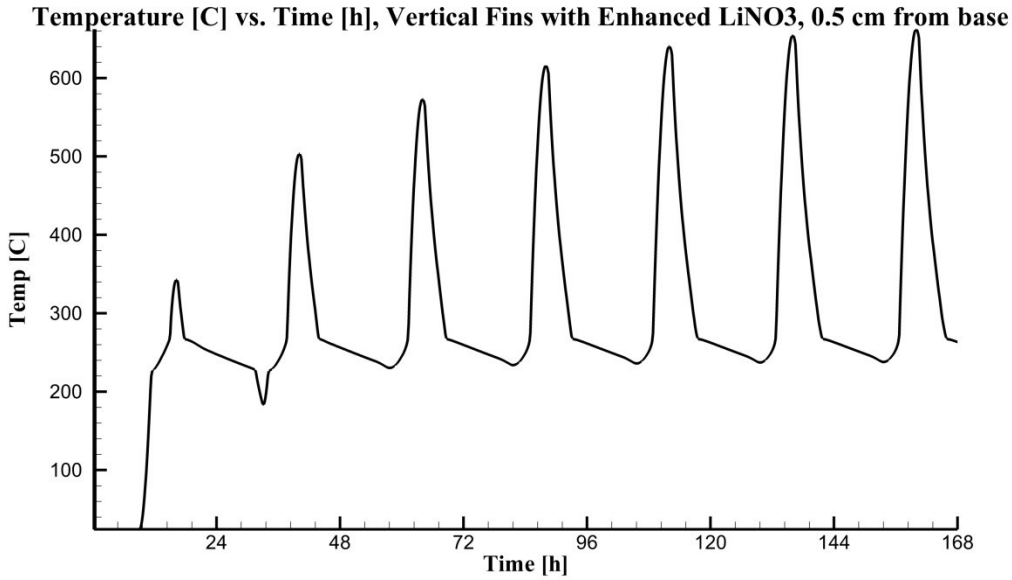

Figure 5.24. Vertical Fins with Enhanced LiNO3 Base Temperature

By comparing the figures, there is essentially no difference between the standard vertical fins model and that with the enhanced Lithium Nitrate. Thus, when constructing a physical model, it would not be necessary to try to increase the thermal conductivity.

5.4 Optimization

The final approach for energy storage in particular was to try to design a model that excelled at energy storage. The goal was to design something that would be able to cook at as close to the ideal cooking range (200 to 250 [C]) as possible. The main issue in previous models was that the evening cooking session started too hot. Granted, without modeling losses from the cooking surface during the day, there is a certain inaccuracy involved with previous attempts.

The approach taken in the optimized energy storage model was to try to allow the cooking surface to get locally hot. In other words, one could take advantage of the poor thermal conductivity of the Lithium Nitrate, allowing the temperatures near the cooking

surface to spike during the day, then hope that the spike will drop out during the two and a half hours before evening cooking. Thus, the model presented in Figure 5.25 was born.

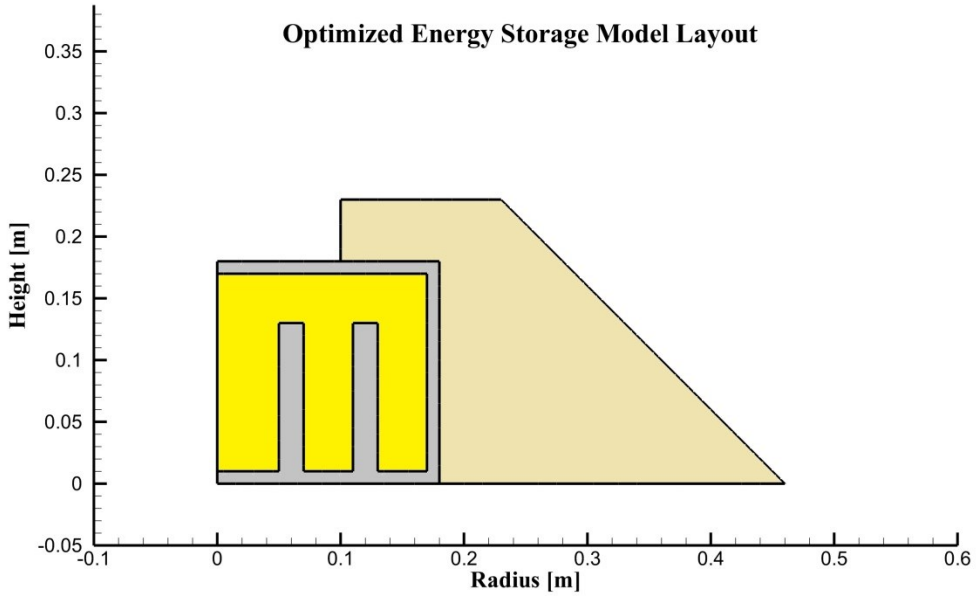

Figure 5.25. Optimized Energy Storage Model Layout

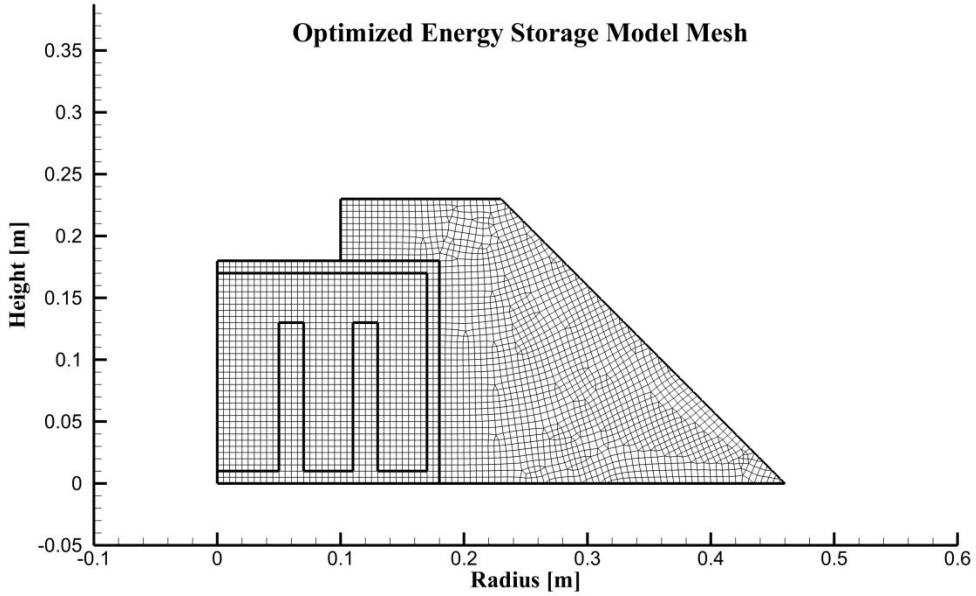

Figure 5.26. Optimized Energy Storage Model Mesh

Figures 5.27 and 5.28 show the surface and base temperatures for the model, respectively. As was discussed with Figure 5.11, the temperature rise actually appears to be in two distinct phases, most obvious in the second day of heating. When cooling in the late afternoon and early evening, the two phases appear again and actually force the user to cook at a higher temperature than desired. Instead of beginning the cooking session at around 240 [C], the temperature was closer to 390 [C]. Table 5.1 shows how the optimized design stacks up against the other six models.

Table 5.1. Evening cooking starting temperature at steady state

Model	**Starting Temperature [C]**
Optimized Storage	409
Aluminum	437
Lithium Nitrate	402
Enhanced Lithium Nitrate	354
Horizontal Fins	421
Vertical Fins	401
Vertical Fins with Enhanced Lithium Nitrate	396

As it turns out, the optimized storage design did not perform significantly better or worse than the other models. The enhanced lithium nitrate did set itself apart in this test, with a starting temperature of around 50 degrees cooler than the other models. Ultimately, because the simulations didn't account for losses off the top during the heating sessions, the initial temperatures were grossly exaggerated and inaccurate. So, while the enhanced lithium nitrate exhibits a lower evening cooking temperature than the other models, it also peaked at over 800 [C] in the late afternoon, according to the

simulations. In the simulations, the energy was continued to be forced into the storage block clear up until 4:30pm, regardless of the temperature of the cooking surface. In a real model, the excessive temperatures of the cooking surface would lead to energy losses. Given the similar performances of the various models, the primary concern should be for cost. The design needs to have some way to transport the energy throughout the storage device – whether by 'enhancing' the Lithium Nitrate with shards of aluminum or by using fins.

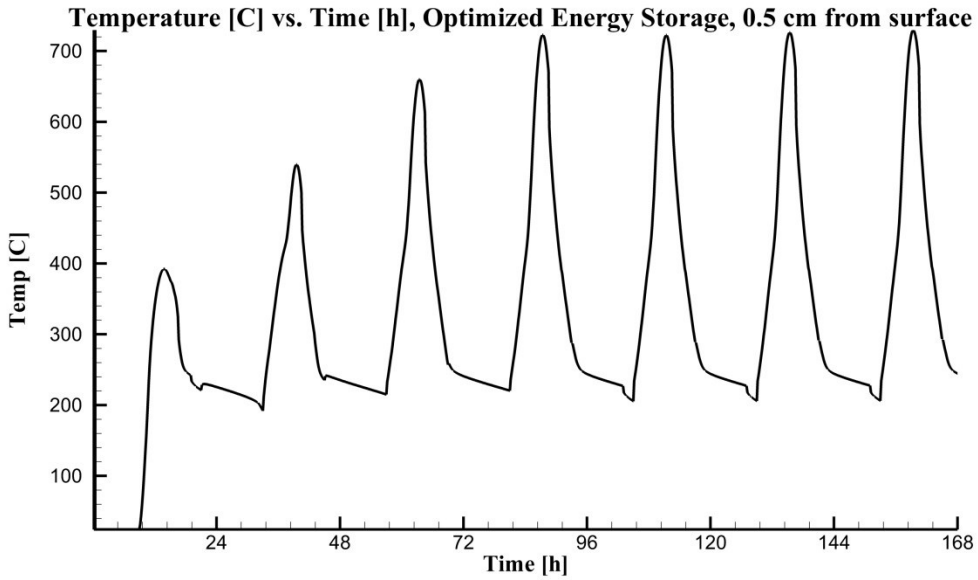

Figure 5.27. Optimized Energy Storage Surface Temperature

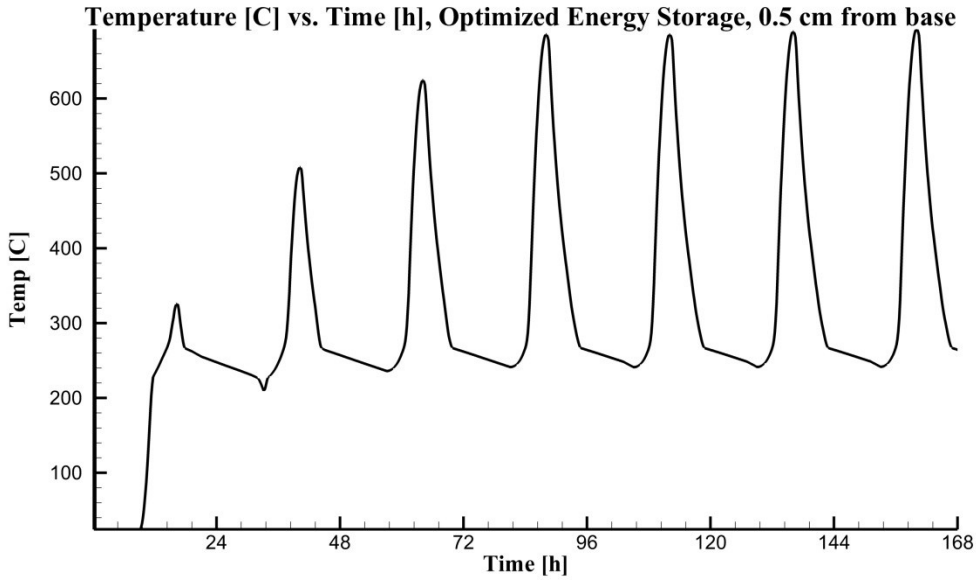

Figure 5.28. Optimized Energy Storage Base Temperature

The final goal was to design a model that excelled at delivering energy. The previous models listed had large temperature drops during their morning cooking sessions. In order to maintain a constant temperature, the new design would need to have plenty of Lithium Nitrate in order to take advantage of the phase change properties. On the other hand, it also had to be able to deliver that energy very quickly to avoid any sort of drop off in cooking surface temperature. Said another way, it needed a lot of stored energy, and it needed to be able to access it very quickly. Figures 5.29 and 5.30 show the layout and mesh for the proposed delivery mechanism. The design has a two centimeter thick cooking surface, one centimeter thick channels of Lithium Nitrate, and half centimeter thick aluminum fins. In order to compare the models equally, they were analyzed for the morning cooking session on the seventh day, which was considered steady state. Neither the aluminum nor lithium nitrate models were warm enough to cook on the seventh morning. Figures 5.31 shows the temperature drop achieved during the morning cooking session on the seventh day.

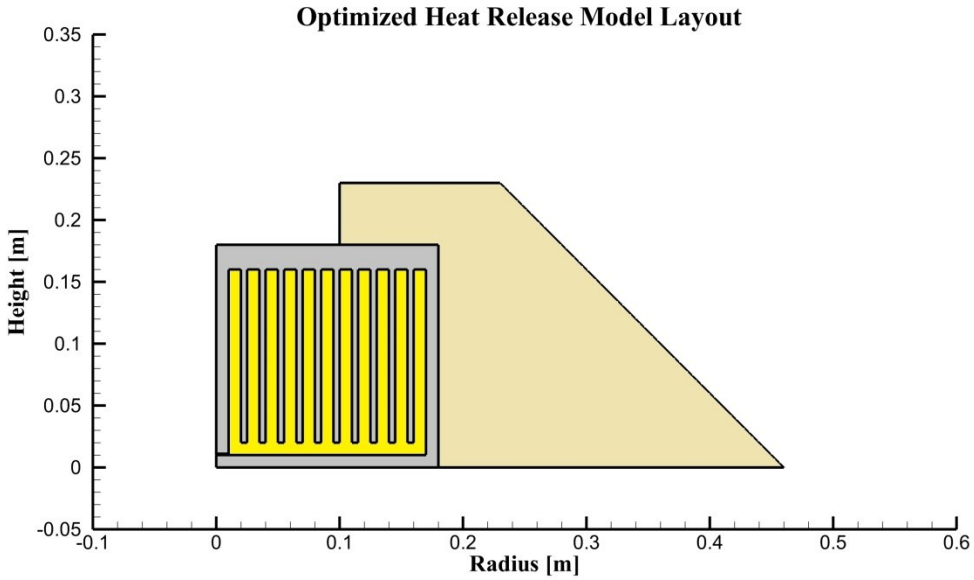

Figure 5.29. Optimized Heat Release Model Layout

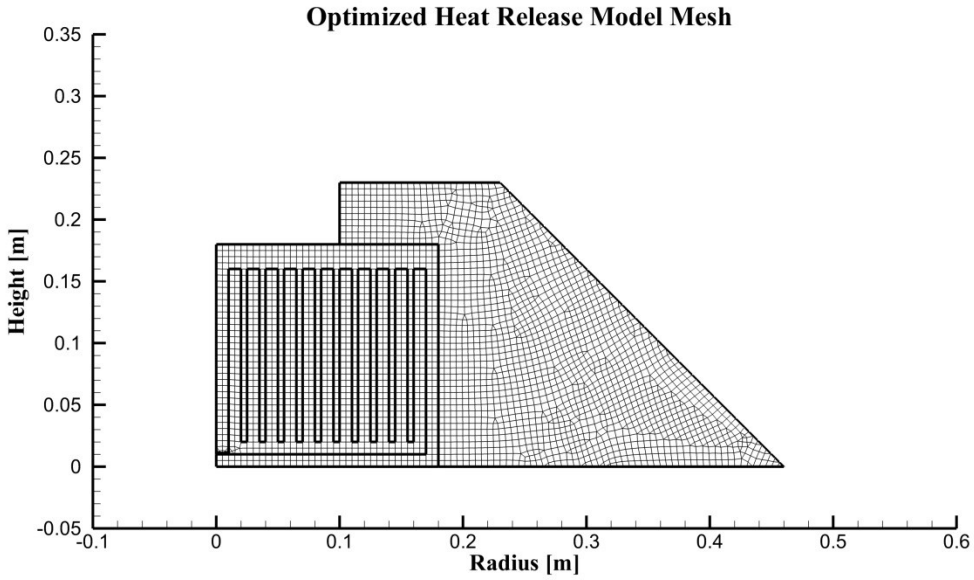

Figure 5.30. Optimized Heat Release Model Mesh

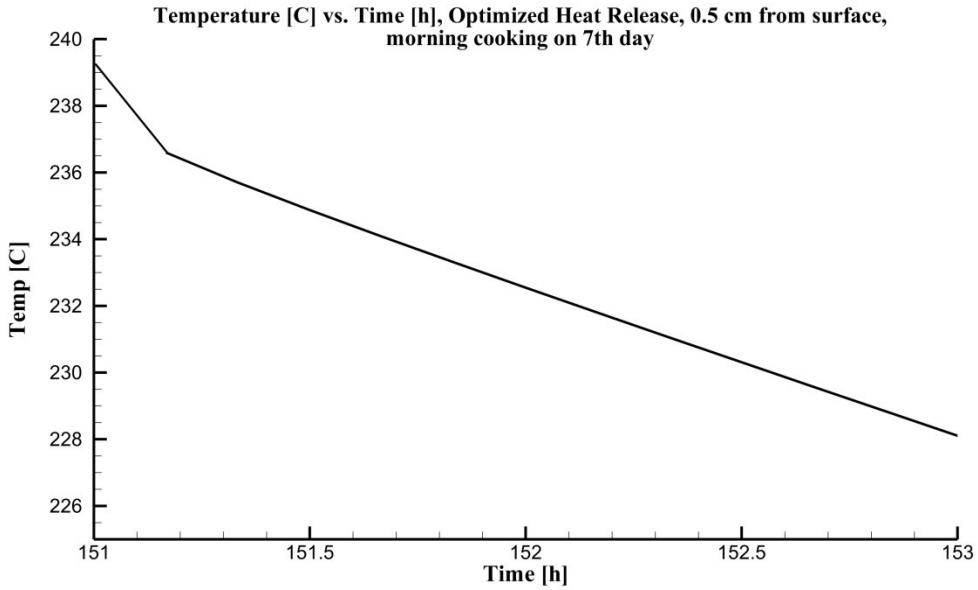

Figure 5.31. Optimized Heat Release Surface Temperature

Table 5.2 summarizes the results for the eight storage designs. As one will notice, the 'optimized' design did not win this study either. Again, the vertical fins with enhanced lithium nitrate performed well. The optimized delivery was not designed with the enhanced lithium nitrate, simply because it would be nearly impossible to improve the lithium nitrate given the strict design constraints presented by such narrow fins and gaps between fins.

Table 5.2. Temperature changes for steady state cooking

Model	**Starting Temperature [C]**	**Finishing Temperature [C]**	**Change in Temperature [C]**
Optimized Delivery	239.2	228.1	11.1
Optimized Storage	228.1	206.8	21.3
Aluminum	215.8	N/A	N/A
Lithium Nitrate	221.3	N/A	N/A
Enhanced Lithium Nitrate	234.2	220.5	13.7
Horizontal Fins	230.6	212.0	18.6
Vertical Fins	235.5	222.2	13.3
Vertical Fins with Enhanced Lithium Nitrate	239.2	228.5	10.7

5.5 Mesh and Time Dependency Checks

Several tests were performed in order to verify that the mesh was dense enough and that the time steps were not too large. The first test was to halve the grid spacing for the aluminum model. Figure 5.32 shows the new mesh density.

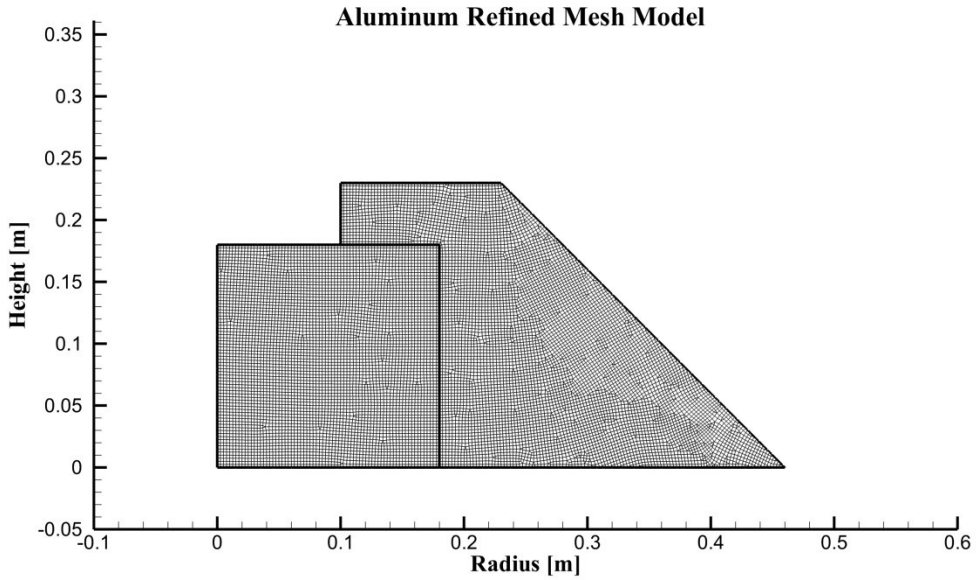

Figure 5.32. Aluminum Refined Mesh Model

Using the exact same boundary and initial conditions, a full seven day simulation was performed in order to compare the original aluminum case to the refined mesh. Figure 5.33 shows the surface temperature for the refined case. The peak temperature reached during the heating session on the seventh day was 537 [C] for both models, thus verifying that they are in agreement.

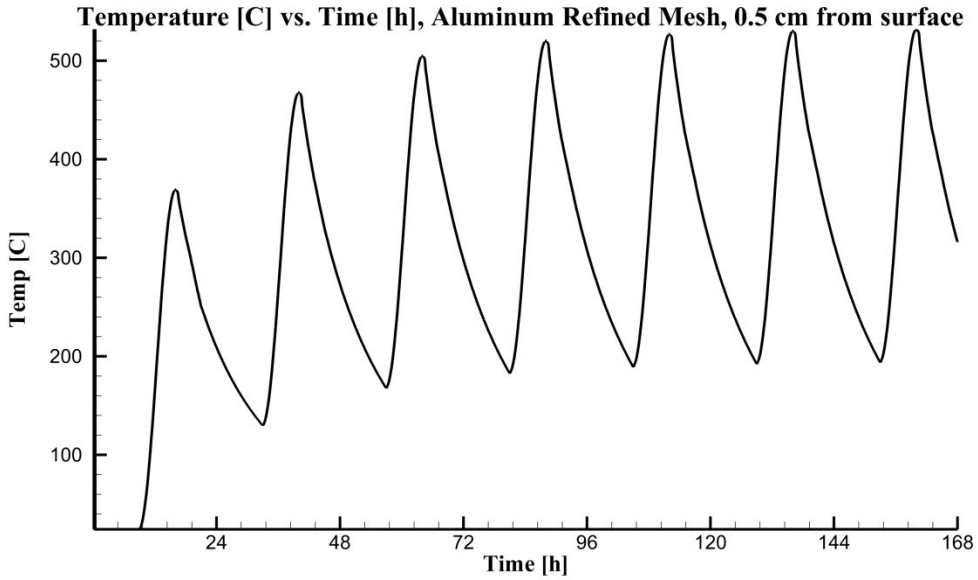

Figure 5.33. Aluminum Refined Mesh Surface Temperature

The next test to perform was a mesh dependency test for the vertical fins model. Figure 5.34 shows the new mesh, while Figure 5.35 shows the surface temperature plot.

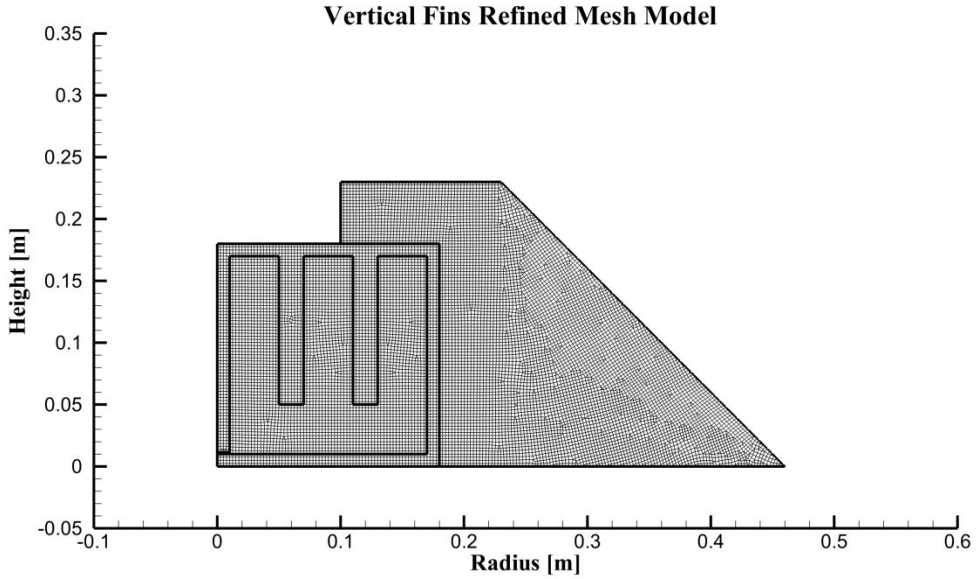

Figure 5.34. Vertical Fins Refined Mesh Model

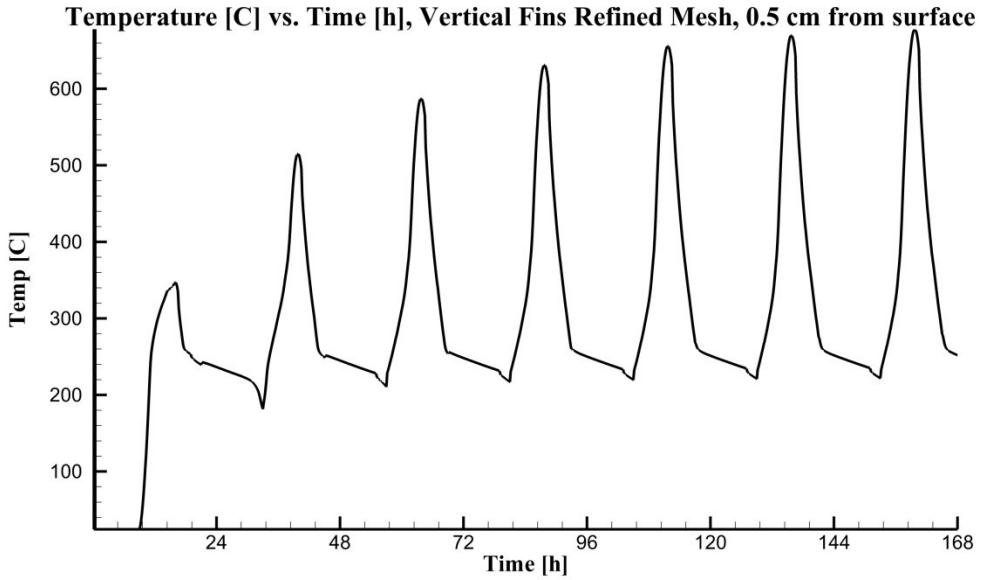

Figure 5.35. Vertical Fins Refined Mesh Surface Temperature

For the refined model, it had a peak temperature of 679 [C] on the seventh day. The original mesh had a peak temperature of 680 [C]. With such a minimal difference, it would have been a waste of computing resources to attempt to further refine the grid. Original computing time was between four and six hours per simulation; the refined models added an hour to the original time.

Finally, a check was performed to see if smaller time intervals would have an impact on the simulations. For the aluminum model, the peak temperature on the seventh day was 537 [C] using time steps of 30 seconds. When the steps were cut to 15 seconds each, the peak remained at 537 [C].

Because mesh and time dependency tests were performed after the original data was gathered, the mesh density and time step sizes were not optimized. Future studies should perform the mesh and time tests before gathering data in order to optimize computing resources.

CHAPTER 6
FUTURE WORK AND RECOMMENDATIONS

6.1 Future Work and Recommendations

The most obvious and pressing problem was to find a nice way to model the losses from the surface during the heating. One possible and simple approach would be to add a curve approximately one millimeter away from the cook surface. This curve can have a heat influx boundary condition applied to it while the actual cook surface can be used with a mixed (radiation and convection) boundary condition. Without future simulations that actually model the losses, it is difficult to make an accurate prediction of which physical model to build.

One thing is for certain: future designs need to include a phase change material, but must also include a method for transferring the energy to the cooking surface. The tests performed in this study showed that the energy storage properties of Lithium Nitrate allow for cooking at or very near the desired cooking temperature. Thus, Lithium Nitrate makes an excellent candidate for storage material. Future tests should include a wider range of materials, including possible salts such as Potassium Nitrate and Sodium Nitrate.

Additional tests need to be performed to check the effects of different sizes of storage material, as well as different configurations for the aluminum. The tests offered in this study are by no means a complete list. Further, the Lithium Nitrate was modeled without natural convection to aid in the dispersal of energy.

Although the research performed was an initial study, it should serve to pave the way for future tests and studies as we inch closer towards the goal of a sustainable cooking method for the villagers of Rajasthan.

REFERENCES

Engineering Toolbox. *Emissivity Coefficients of some common Materials.* 2012. http://www.engineeringtoolbox.com/emissivity-coefficients-d_447.html (accessed March 15, 2013).

Jha, S., and A. Singh. "Physical and Thermal Properties of Untreated and Chemically Treated Rice Husk." *Journal of Agricultural Engineering*, 2007: 44.

Juliano, Bienvenido. "Rice: Chemistry and Technology." In *Rice: Chemistry and Technology*, edited by Bienvenido Juliano, 696. St. Paul, MN: The American Association of Cereal Chemists, 1985.

Kenisarin, Murat M. "High-temperature phase change materials for thermal energy storage." *Renewable and Sustainable Energy Reviews*, 2009: 955-970.

Mani, Anna, and S. Rangarajan. *Solar Radiation over India.* Book, New Delhi: Allied Publishers Private Limited, 1982.

PBS. *Finding the Focal Point.* 2013. http://www.pbs.org/wgbh/nova/education/activities/3406_solar_03.html (accessed March 27, 2013).

Scheffler, Wolfgang. *Solare Bruecke.* 2013. http://www.solare-bruecke.org/ (accessed March 15, 2013).

Wikipedia. *Rajasthan.* April 14, 2013. http://en.wikipedia.org/wiki/Rajasthan (accessed April 25, 2013).

World Health Organization. *World Health Organization Fact Sheet Number 292.* September 2011. http://www.who.int/mediacentre/factsheets/fs292/en/ (accessed March 20, 2013).